

Cardiac repolarization analysis using the surface electrocardiogram

BY ESTHER PUEYO^{1,2,*}, JUAN PABLO MARTÍNEZ^{1,2} AND PABLO LAGUNA^{1,2}

¹*Communications Technology Group, Aragon Institute for Engineering Research (I3A), University of Zaragoza, 50018 Zaragoza, Spain*

²*CIBER de Bioingeniería, Biomateriales y Nanomedicina (CIBER-BBN), 50018 Zaragoza, Spain*

Sudden cardiac death (SCD) is a challenging health problem in the western world. Analysis of cardiac repolarization from the electrocardiogram (ECG) provides valuable information for stratifying patients according to their risk of suffering from arrhythmic events that could end in SCD, as well as for assessing efficacy of antiarrhythmic therapies. In this paper, we start by exploring the cellular basis of ECG repolarization waveforms under both normal and pathological conditions. We then describe basic preprocessing steps that need to be accomplished on the ECG signal before extracting repolarization indices. A comprehensive review of techniques aimed to characterize spatial or temporal repolarization dispersion is provided, together with a summary of their usefulness for clinical risk stratification. Techniques that describe spatial dispersion of repolarization are based on either differences in repolarization duration or T-wave loop morphology. Techniques that evaluate temporal dispersion of repolarization include the analysis of QT interval adaptation to heart rate changes, QT interval and T-wave variability, and T-wave alternans.

Keywords: electrocardiogram; repolarization; dispersion; arrhythmia

1. Introduction

Sudden cardiac death (SCD) is one of the major health problems in industrialized countries. Its incidence is similar in all western populations, where estimates indicate that 1 out of 1000 subjects dies every year due to SCD (Smith & Cain 2006). This represents approximately 20 per cent of all deaths and highlights the importance of developing strategies to prevent SCD. SCD is defined as death resulting from the abrupt loss of heart function that occurs unexpectedly and within a short time after symptoms appear (American Heart Association 2007, www.americanheart.org). Most SCDs result from ventricular arrhythmias such as ventricular tachycardia (VT) or ventricular fibrillation (VF), while only in a small number of cases is SCD caused by bradycardia (American Heart Association 2007, www.americanheart.org).

*Author and address for correspondence: Communications Technology Group, Aragon Institute for Engineering Research (I3A), University of Zaragoza, 50018 Zaragoza, Spain (epueyo@unizar.es).

One contribution of 13 to a Theme Issue ‘Signal processing in vital rhythms and signs’.

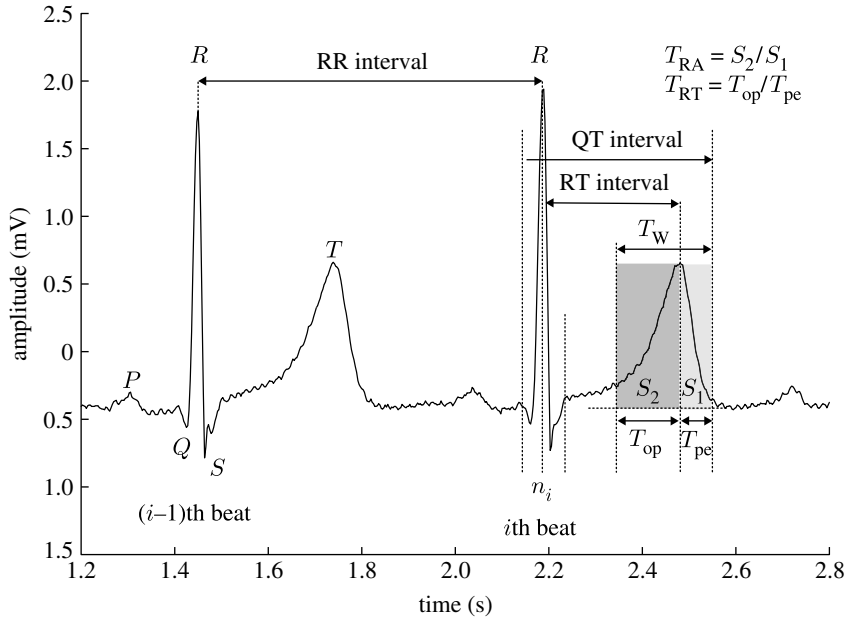


Figure 1. Most relevant waveforms of the ECG, and parameters of interest on it.

As pointed out in different studies, there are three fundamental factors involved in the initiation and maintenance of arrhythmias: a vulnerable myocardium; triggers; and modulators. A vulnerable myocardium is the substrate for arrhythmogenesis, in the sense that when triggering factors act on it they are able to precipitate malignant arrhythmias that may lead to SCD. Factors that modulate the arrhythmogenic substrate or the triggers play their role in altering the electrophysiological properties of the heart. Among those modulators, an important one is the autonomic nervous system (ANS; Coumel 1993).

Therapeutic options are to a large extent conditioned by the factors (substrate, triggers and modulators) that contribute to arrhythmia generation. Implantable cardioverter defibrillators have been shown to be highly effective in treating VT and VF by applying a shock to the heart that restores its sinus rhythm. Also, antiarrhythmic drugs can act to lower the number of SCDs by preventing the occurrence of arrhythmias. Genetic and genomic therapies are currently being explored in animal experiments with promising results. The use of a therapy or a combination of therapies needs to be assessed regarding their safety and cost-effectiveness. Strategies for identification of high-risk patients who would benefit from a specific therapy are therefore necessary.

Repolarization analysis from the surface electrocardiogram (ECG) has proved to be useful for risk assessment, with the additional advantage of being applicable to the general population (American Heart Association 2007, www.americanheart.org). In figure 1, a cardiac cycle is shown together with the definitions of the most relevant ECG waves. For ECG genesis, see Malmivuo & Plonsey (1995).

In §2, the ionic and cellular basis of ECG repolarization waveforms under both normal and pathological conditions is depicted. In §3, basic concepts of ECG signal processing are described. In §4, ECG measures describing spatial characteristics of ventricular repolarization are reviewed, including those that

evaluate dispersion of repolarization from either ECG intervals or T-wave loop morphology. In §5, ECG measures describing temporal variations of repolarization shape or duration are examined, including T-wave alternans (TWA), dynamicity of QT dependence on heart rate (HR) and QT and T-wave variability.

2. Ionic basis of repolarization and cardiac arrhythmias

(a) Repolarization waveforms

(i) Membrane currents and action potential

The study of the relationship between ECG waveforms and action potential (AP) properties of individual cardiac cells is fundamental for a better understanding of the mechanisms involved in the genesis of arrhythmias. The AP associated with each cardiac cell is the result of ion charges moving in and out of the cell through voltage-gated channels. A representative AP of a ventricular myocyte is presented in figure 2a. At rest, the membrane potential, i.e. the voltage difference between the inside and the outside of the cell, is between -90 and -80 mV. When the cell is excited by a sufficiently large stimulus, ions start to flow through channels to which they are permeable and there is an increase of the membrane potential (the cell depolarizes). The initial fast upstroke (phase 0) of the AP is due to a transient increase in the inward fast sodium channel I_{Na} (figure 2b). Following phase 0, there is an early but brief repolarization (phase 1) caused by a transient outward potassium current, I_{to} . This current, which is differently expressed across the heart, gives the AP its spike-and-dome morphology. In phase 2, the influx of calcium through the L-type calcium channel (I_{CaL}) compensates the repolarizing currents, delaying repolarization and creating a slow-decaying plateau. During phase 3, potassium currents, mainly the delayed rectifier currents, I_{Kr} and I_{Ks} , and the inward rectifying current, I_{K1} , lead the cell to its resting state. The cell remains in this state (phase 4) until a new stimulus excites it. In addition to the named ion channels, electrogenic transporters, such as the sodium–potassium pump (I_{NaK}) or the sodium–calcium exchanger (I_{NaCa}), contribute to AP generation, being both involved in the transportation of ions necessary to maintain the ionic balance of the cell membrane.

(ii) Intrinsic heterogeneities

APs of all the cells in the heart are not identical. Differences exist in ionic current expressions of, for example, nodal, atrial and ventricular cells. Heterogeneities can be found not only between different cardiac chambers, but also within each chamber. Whereas depolarizing currents are quite uniform throughout the heart, differences in repolarizing currents have been documented between anterior, inferior and posterior walls of the left ventricle, and also between the apex and the base (Kuo & Surawicz 1976). Transmural differences exist as well, with at least three types of cells recognized in the ventricle: endocardial; mid-myocardial; and epicardial. Those intrinsic heterogeneities are necessary for cardiac function under normal physiological conditions.

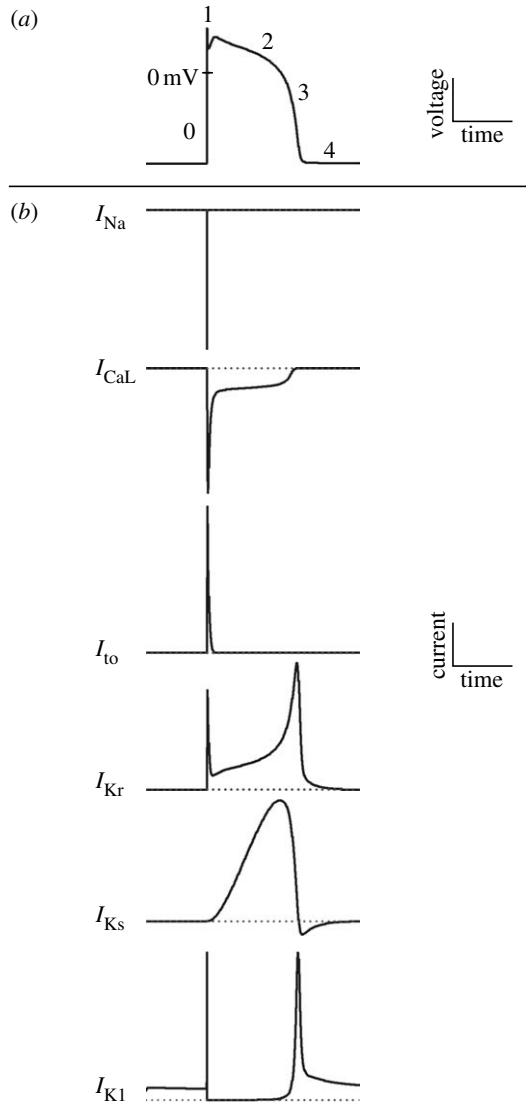


Figure 2. (a) AP of a ventricular myocyte, with indication of its phases. (b) Ionic currents underlying the different AP phases are illustrated.

(iii) *Genesis of ECG repolarization waves and intervals*

The T wave of the ECG is mainly an expression of heterogeneity of ventricular repolarization. The formation of the T wave is dependent on both the sequence of ventricular activation and the heterogeneities in AP characteristics throughout the ventricular myocardium. Changes in the shape and duration of the T wave have been studied under a variety of conditions with the purpose of understanding the underlying ionic changes (Gima & Rudy 2002). Other ECG repolarization waves are the J wave, the ST segment and the U wave. Additionally, the QT interval, measured in the ECG from the onset of the QRS

complex to the end of the T wave, has been widely used in repolarization studies. It represents the time needed for depolarization plus repolarization of all the cells in the ventricular myocardium.

(b) *Cardiac arrhythmias*

(i) *Pathological heterogeneities*

Intrinsic heterogeneities in ventricular repolarization are accentuated under different pathological states, including ischaemia, Brugada syndrome, long-QT syndrome (LQTS), heart failure, arrhythmogenic right ventricular dysplasia or ventricular hypertrophy. In §4a, methods to quantify dispersion of repolarization from surface ECG time intervals are described. Also, amplified heterogeneities in AP repolarization throughout the ventricular myocardium, potentially in a non-homogeneous way, are known to be reflected in strong T-wave morphology changes. In §4b, several indices used to measure electrocardiographic T-wave morphology changes are reviewed.

In addition to spatial heterogeneities, augmented temporal (i.e. across beats) repolarization heterogeneities have also been associated with the occurrence of arrhythmic events. As an example, abnormal APD adaptation in response to cycle length changes has been shown to play a role in the genesis of arrhythmias (Carmeliet 2006). Approaches for assessment of repolarization adaptation to HR changes from the surface ECG are described in §5a. Also, there is growing evidence that AP instability, measured as fluctuations in the duration of the AP, is closely linked to SCD in different settings (Hondeghe *et al.* 2001). Quantification of QT variability can be considered as an approximation to the study of such phenomena, and is explored in §5b. Finally, §5c examines TWA, which have been proposed as a surrogate of proarrhythmia in a variety of studies (Narayan 2006b). Cellular basis for TWA can be found in AP alternans, defined as changes in AP occurring on an every-other-beat basis (Pastore *et al.* 1999). Concordant alternans develop if all cells alternate in an almost synchronized way. Certain conditions, such as ischaemia, extrasystoles or a sudden HR change, may reverse the phase of alternans regionally, causing discordant alternans and unidirectional block, and setting the stage for the onset of malignant ventricular arrhythmias such as VF (Pastore *et al.* 1999).

Analysis of cardiac arrhythmias, either at the cellular level or from the surface ECG, should start by identifying the mechanisms contributing to them. Cardiac arrhythmias can be due to abnormalities in impulse formation and/or impulse conduction.

(ii) *Abnormalities of impulse generation*

Automaticity. Under normal conditions, the SA node is the prevailing pacemaker of the heart. Abnormal automaticity occurs when other cells, such as cells in the atrioventricular node or in the conduction system, undertake the SA node function. Ventricular cells may even be converted to pacemaker cells under states in which I_{K1} , the current that maintains the resting membrane potential, becomes downregulated (Akar & Tomaselli 2004). Certain forms of VT arise due to such abnormalities.

Afterdepolarizations and triggered activity. Even in the case of normal SA node functioning, some cells can develop rates of firing faster than that of the SA node. New APs are initiated in those cells and their adjacent ones independently of the SA node. This triggered activity arises due to the formation of afterdepolarizations, which are second depolarizations that occur during repolarization of the AP, so-called early afterdepolarizations (EADs), or after repolarization of the AP, so-called delayed afterdepolarizations (DADs). Several studies have pointed to EADs playing a role in the initiation and perpetuation of torsades de pointes (TdP; Lawrence et al. 2005). TdP is a polymorphic VT that can degenerate into fibrillation and SCD (Dessertenne 1966).

(iii) *Abnormalities of impulse conduction*

Abnormal impulse conduction results in re-entry, which describes the fact that a circuitous wavefront re-excites the same tissue indefinitely, as opposed to normal conditions where all tissue is excited only once. For re-entry to occur, two conditions are needed: unidirectional conduction block and slow conduction, allowing each site to recover before re-excitation. The obstacle around which the wavefront travels during re-entry may be anatomic (such as infarct scar) or functional (such as a region of conduction block). VF is an example of functionally determined re-entrant arrhythmia.

3. ECG preprocessing for repolarization analysis

We can discern four main tasks before computing the ECG repolarization indices. *ECG filtering and preconditioning.* This includes removal of muscle noise, powerline interference and baseline wander (Sörnmo & Laguna 2005). The digitized ECG signal recorded in lead l , after filtering, is denoted by $x_l(n)$, while vector $\mathbf{x}(n) = [x_1(n), \dots, x_L(n)]^T$ is used for the multilead filtered signal.

QRS detection. Beat, QRS, detection is a necessary step before any beat analysis (Sörnmo & Laguna 2005). It provides a series of samples n_i , and its related RR intervals $RR_i = n_i - n_{i-1}$, $i = 0, \dots, B$, corresponding to the detected QRS complexes.

Wave delineation. Automatic wave delineation, i.e. determination of the wave boundaries and peaks within the cardiac beat, is an important task since essential diagnostic information is known to be contained in the waves' amplitudes and durations of a heartbeat (figure 1). The most relevant points for repolarization analysis are the QRS boundaries, T-wave boundaries and T-wave peak. Some intervals characterizing repolarization in each beat are the QT interval (QT_i between the QRS onset and the T-wave end), RT interval (RT_i , between the QRS fiducial point and the T-wave peak), T-wave width (T_{w_i}) and T-wave peak-to-end (T_{pe_i}).

Different delineation approaches can be found in the literature. Multiscale analysis based on the dyadic wavelet transform, allowing representation of a signal's temporal features at different resolutions, has proven to be very suitable for QRS detection and delineation of ECG waves (Martínez et al. 2004).

Determination of the onset and the end of cardiac phenomena based on the partial view given by a single lead is intrinsically limited, as discussed in Malik (2004). Thus, there is a current interest focusing on multilead delineation.

Multilead methods, based on either selection rules applied to single-lead delineation results or VCG processing, have shown improved accuracy and stability (Almeida *et al.* 2006; Martínez *et al.* 2007).

Segmentation. Computation of most ECG indices requires identification and extraction of the ventricular repolarization phase (the ST–T complex) of each beat. A repolarization segmentation window W_i is established, usually beginning at fixed or RR-dependent offsets from the QRS fiducial point or the QRS end. In addition, an alignment stage can be subsequently used if better beat-to-beat synchronization is required. If an N -sample window, W_i , beginning at sample n_i^w is defined for each beat and defines the repolarization window, the extracted repolarization segment for the i th beat and l th lead can be denoted as $x_{i,l}(n) = x_l(n_i^w + n)$, $n = 0, \dots, N - 1$. For multilead analysis, the $L \times 1$ vector $\mathbf{x}_i(n) = [x_{i,1}(n), \dots, x_{i,L}(n)]^T$ contains the samples at the different leads.

4. Spatial ECG repolarization indices for risk stratification

In this section, a review of ECG indices proposed in the literature to assess spatial heterogeneity of ventricular repolarization is presented, together with their value for assessing the risk of suffering from malignant ventricular arrhythmias.

(a) Dispersion of repolarization reflected on ECG intervals

Interlead QT dispersion (QT_d), measured as the difference between maximum and minimum QT values (Day *et al.* 1990) or as QT standard deviation in the 12 standard leads, was proposed as an index to assess ventricular repolarization dispersion (VRD). QT_d was proposed as a regional marker of VRD, considering that each ECG lead mainly records the local activity at different myocardium areas. This measure was claimed to be correlated with APD dispersion in animals and humans (Zabel *et al.* 1998). However, Malik *et al.* (2000) have shown that the measurement might be affected by inaccuracies in the determination of the T-wave end, the existence of U waves or notched T waves. QT_d is significantly different between patients with a wide and a narrow T-wave loop, and a correspondence has been observed between QT_d and the T-wave loop morphology (Kors *et al.* 1999) rather than with VRD. In addition, similar QT_d values have been measured on the standard 12-lead ECG and on synthesized 12 leads from the orthogonal XYZ leads, which intrinsically leave out regional repolarization heterogeneity (Macfarlane *et al.* 1998). As a result, this QT_d concept has been largely abandoned as a marker of VRD.

Other authors used isolated, perfused canine hearts to measure QT_d and T-wave width, T_W , from the root-mean-square (r.m.s.) curve obtained from the following: the available epicardial electrograms; ECG body surface leads; standard precordial ECG leads; and optimal lead set (Fuller *et al.* 2000). They induced myocardial repolarization dispersion by changing temperature, cycle length and activation sequence. VRD, which was measured directly using recovery times from epicardial potentials, was compared with T_W and QT_d . VRD was strongly correlated with T_W , but not with the classical QT_d . This hypothesis on T_W as a measure of repolarization dispersion was also verified in a rabbit heart model where increased dispersion was generated by D-sotalol

and premature stimulation (Arini et al. 2008). T_W is a complete measure of dispersion as evidenced on the ECG, but studies show that transmural dispersion is preferentially expressed by the distance from T peak to T end, T_{pe} , thus suggesting this parameter as a transmural dispersion index (Zareba et al. 2000). In addition, when addressing the problem of evaluating T_W in recordings under ischaemia, the T onset estimation can vary largely with the ST elevation, making T_W estimation unsafe, and then T_{pe} being a better alternative (Arini et al. 2006).

(b) *Dispersion of repolarization reflected on T-wave morphology*

Based on the idea that the larger the dispersion, the more complexity in the T wave will appear, several indices trying to describe the T-wave shape have been derived. These efforts resulted in some techniques based on principal component analysis (PCA), whose aim was to extract valuable information from the T-wave shape (Badilini et al. 1995; Priori et al. 1997).

The total cosine R-to-T descriptor, T_{CRT} , is defined as the cosine angle between the dominant vectors of depolarization and repolarization as measured in a three-dimensional loop and has been well validated as an index of mortality (Acar et al. 1999; Smetana et al. 2004a,b). The transformed leads are $\mathbf{w}_i(n) = [w_{i,1}(n) \ w_{i,2}(n) \ \dots \ w_{i,L}(n)]^T$, where

$$\mathbf{w}_i(n) = \mathbf{V}_i^T \mathbf{x}_i(n), \quad (4.1)$$

with \mathbf{V}_i being an $L \times L$ matrix whose columns are the eigenvectors of the interlead autocorrelation matrix for beat i . The first three principal components of the L leads are taken to eliminate the interlead correlation and to form the dipolar signal $\mathbf{w}_{i,D}(n) = [w_{i,1}(n) \ w_{i,2}(n) \ w_{i,3}(n)]^T$, where the autocorrelation matrix has been estimated from the complete heartbeat and the transformed signal $\mathbf{w}_{i,D}(n)$ also includes the complete heartbeat, i.e. the PQRST complex (Castells et al. 2007). A 30 ms window (N_{QRS} samples) is defined centred around the QRS fiducial point n_i . The T-wave peak position, $n_{i,T}$, is estimated as the position in the ST-T complex with maximum $|\mathbf{w}_{i,D}(n)|$. Then, the index T_{CRT_i} is defined by

$$T_{CRT_i} = \frac{1}{N_{QRS}} \sum_{n=0}^{N_{QRS}-1} \cos \angle(\mathbf{w}_{i,D}(n), \mathbf{w}_{i,D}(n_{i,T})). \quad (4.2)$$

When a comparison of the ventricular gradient is to be made from beats at different stages of the same recording, hypothesizing that only the T vector changes with repolarization heterogeneity, the gradient can be estimated with respect to a fixed reference, reducing the uncertainty in estimating the depolarization reference (Arini et al. 2008). This reference \mathbf{u} can be taken to be the dominant direction, $\mathbf{u} = [1 \ 0 \ 0]^T$, of the dipolar decomposition at a control situation, and is then called ‘total angle principal component-to-T’, T_{PT} , having the form

$$T_{PT_i} = \angle(\mathbf{u}, \mathbf{w}_{i,D}(n_{i,T})). \quad (4.3)$$

Another repolarization index is the total morphology dispersion, T_{MD} , computed by first reconstructing the original signal leads after truncating to the dipolar components. This is done by splitting $\mathbf{V}_i = [\mathbf{V}_{i,3} \ \mathbf{V}_{i,L-3}]$

and obtaining

$$\hat{\mathbf{x}}_i(n) = \mathbf{V}_{i,3} \mathbf{V}_{i,3}^T \mathbf{x}_i(n). \quad (4.4)$$

This new signal $\hat{\mathbf{x}}_i(n)$ is again processed to produce an SVD-decomposed signal, but now restricted to the ST–T segment, obtaining the transformation matrix $\check{\mathbf{V}}_i$ from which we concentrate on the first two transformed leads, $\check{\mathbf{V}}_{i,2}$, assumed to contain the most important information of the ST–T segment. By analysing the reconstruction equation in (4.4), now applied to $\check{\mathbf{V}}_{i,2} \check{\mathbf{x}}_i(n) = \check{\mathbf{V}}_{i,2} \mathbf{V}_{i,2}^T \hat{\mathbf{x}}_i(n)$, it is obvious that $\check{\mathbf{V}}_{i,2} = [\phi_{i,1} \ \cdots \ \phi_{i,L}]^T$, where $\phi_{i,l}$ are the 2×1 reconstruction vectors that can be interpreted as the direction into which the SVD-transformed signal needs to be projected to recover each original lead in $\check{\mathbf{x}}_i(n)$. The angle between two directions, relative to each pair of leads l_1 and l_2 , can then be calculated as

$$\alpha_{l_1, l_2}(i) = \angle(\phi_{i, l_1} \phi_{i, l_2}) \in [0^\circ, 180^\circ], \quad (4.5)$$

thus measuring the difference in shape between leads l_1 and l_2 (a small angle implies similar shape). The unnormalized T_{MD_i} index is defined as

$$T_{\text{MD}_i} = \frac{1}{L(L-1)} \sum_{\substack{l_1, l_2=1 \\ l_1 \neq l_2}}^L \alpha_{l_1, l_2}(i), \quad (4.6)$$

which reflects the mean dispersion in the projection of the repolarization ST–T segment. Originally, T_{MD} was defined with each $\phi_{i,l}$ multiplied by its corresponding eigenvalue (Acar *et al.* 1999); this original definition differs in its geometrical interpretation from the one given in (4.6).

Other measurements are related to the dispersion of the eigenvalues of the interlead repolarization correlation matrix $\hat{\mathbf{R}}_{x_i} = \sum_{n=0}^{N-1} \mathbf{x}(n) \mathbf{x}^T(n)$, denoted as $\lambda_{i,j}$, $j=1, \dots, L$ when sorted in descending order. The sum of the first three eigenvalues represents the energy of the dipolar components of the repolarization, while the rest of eigenvalues represent non-dipolar components. The *T-wave residuum*, T_{WR} , measures the relative energy of the non-dipolar components (Acar *et al.* 1999; Malik *et al.* 2000; Smetana *et al.* 2004a,b),

$$T_{\text{WR}_i} = \sum_{j=4}^L \lambda_{i,j} / \sum_{j=1}^L \lambda_{i,j}. \quad (4.7)$$

The underlying hypothesis is that the electrical dipolar model applies to normal repolarization, and most of the leads can be compactly expressed by the first three components. When it is not the case and local heterogeneities are present at the myocardium, the dipolar model no longer applies and local heterogeneities generate larger dispersion of the eigenvalues. Therefore, an increase in repolarization heterogeneity results in higher T_{WR_i} values. *T-wave complexity*, T_c , defined as

$$T_c = \sum_{j=2}^L \lambda_{i,j} / \sum_{j=1}^L \lambda_{i,j}, \quad (4.8)$$

was introduced to quantify the ST–T waveform shape (Priori *et al.* 1997), although a square root was in the original definition. A T_c value close to 1 means that the loop is highly extended in at least two dimensions. The spatial T-wave complexity has also

been defined as the ratio between the second and the first eigenvalue, $T'_c = \lambda_2/\lambda_1$, with similar geometrical interpretation. It has been shown that T'_c was higher in patients with LQTS than in healthy subjects (Priori *et al.* 1997).

Based on the evidence that repolarization dispersion produced taller and more symmetric T waves (di Bernado & Murray 2000), shape indices have been proposed as markers of arrhythmic risk (Langley *et al.* 2002). Indices such as T-wave amplitude (T_A), the ratio of the areas at both sides of the T peak (T_{RA}) and the ratio of the T-wave times at both sides of the T peak (T_{RT} ; figure 1) have been proposed in the literature and their relationship with HR has been established (Langley *et al.* 2002; Simón *et al.* 2007).

5. Temporal ECG repolarization indices for risk stratification

This section explores ECG indices reported in the literature as descriptors of temporal heterogeneity of ventricular repolarization. Their ability to provide information on the likelihood of suffering from ventricular arrhythmias is reviewed.

(a) QT adaptation to HR changes

The QT interval is influenced by changes in HR, although other factors, such as the direct influence of ANS activity on the ventricular myocardium, also contribute to its determination (Ahnve & Vallin 1982). In order to be able to compare QT measurements obtained at diverse HR ranges, a variety of HR correction formulae have been proposed in the literature to obtain a corrected QT interval (QT_c; Malik 2001). Upper limits for normal QT_c values of 440 ms in men and 460 ms in women have been reported (Yap & Camm 2003). Prolongation of QT or QT_c has been recognized as a risk marker in some studies (Okin *et al.* 2000; Yap & Camm 2003). While this may be true in certain populations, it is today clear that, in general, QT or QT_c prolongation is a poor surrogate for proarrhythmia (Lawrence *et al.* 2005).

Additionally, when analysing ECG recordings with unstable heart rhythm, there is another important (frequently ignored) factor that affects the QT interval, which is its hysteresis lag after HR changes. It is known that the QT interval does not follow cycle length changes immediately, but it requires some time to reach a new steady state. If ambulatory recordings, e.g. 24-hour Holter ECGs, are analysed, methods to characterize QT adaptation should be incorporated into the study. Although a possible alternative would be to discard segments of the recordings presenting unstable heart rhythm, it has been shown in different clinical studies that this is not an adequate option, since important information for prediction of arrhythmias is found in those segments (Malfatto *et al.* 1994). According to some authors, the physiological underpinnings of repolarization adaptation are such that, after a fast increase in HR, they allow a sufficient diastolic filling (during which depolarizing currents can recover from inactivation) at the same time that they prevent a premature ventricular complex from interrupting the T wave, a phenomenon that predisposes to the development of serious ventricular arrhythmias (Padrini *et al.* 1997).

QT hysteresis has been investigated and quantified under various conditions. Lau *et al.* (1988) showed that the ventricular paced QT interval takes between 2 and 3 min to reach 90 per cent of its change secondary to a change in HR, with the time

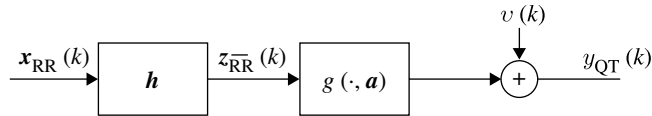


Figure 3. Block diagram used to model the QT/RR relationship (Pueyo *et al.* 2004).

course of adaptation being well approximated by an exponential. They demonstrated that QT requires more time to follow HR decelerations than HR accelerations, but in any case, the adaptation process always showed two phases: a fast initial phase covered in a few tens of seconds, which was followed by a second slower phase that took several minutes to complete. In other studies, QT adaptation was investigated after a provoked HR change or after physical exercise, and a QT lag of some minutes was demonstrated (Sarma *et al.* 1987; Lewis & Short 2006). Fossa *et al.* (2006) investigated QT hysteresis in animal studies using a dynamic beat-to-beat analysis that allows the definition of a normal QT–RR boundary valid under varying autonomic conditions.

In Pueyo *et al.* (2004), a method was proposed to assess and quantify QT adaptation to spontaneous HR changes in Holter ECGs from post-myocardial infarction (MI) patients. The method considers weighted averages of cycle lengths preceding each QT measurement so as to account for QT dependence on HR history. Specifically, the relationship between the QT interval and the RR interval (inverse of HR) is modelled using a system composed of an FIR filter followed by a nonlinear biparametric regression function (figure 3). The input to the system is defined from the resampled beat-to-beat RR_i interval series (denoted by $x_{RR}(k)$, where k is the discrete time), the output is the resampled QT_i interval series ($y_{QT}(k)$) and additive noise $v(k)$ is considered so as to include, for example, delineation and modelling errors. The first (linear) subsystem describes the influence of previous RR intervals on each QT measurement, while the second (nonlinear) subsystem is representative of how the QT interval evolves as a function of the weighted average RR measurement, \overline{RR} , obtained at the output of the first subsystem. The global input–output relationship is thus expressed as

$$y_{QT}(k) = g(z_{\overline{RR}}(k), \mathbf{a}) + v(k), \quad (5.1)$$

where $z_{\overline{RR}}(k) = [1 \quad z_{\overline{RR}}(k)]^T = [1 \quad \mathbf{h}^T \mathbf{x}_{RR}(k)]^T$. In the above expressions,

$$\mathbf{x}_{RR}(k) = [x_{RR}(k) \quad x_{RR}(k-1) \quad \dots \quad x_{RR}(k-N+1)]^T, \quad (5.2)$$

is the history of RR intervals; $\mathbf{h} = [h_0 \quad \dots \quad h_{N-1}]^T$ is the impulse response of the FIR filter; and $g(\cdot)$ is the regression function parametrized by vector $\mathbf{a} = [a_0 \quad a_1]^T$ (see Pueyo *et al.* (2004) for a list of used regression functions). Identification of the unknown system is performed individually for each patient using a global optimization algorithm. According to the results in Pueyo *et al.* (2004), the QT interval requires nearly 2.5 min to follow HR changes, in mean over patients, although both the duration and profile of QT hysteresis are found to be highly individual. In agreement with Lau *et al.* (1988), the adaptation process is shown to be composed of two distinct phases: fast and slow.

The methodology described in Pueyo *et al.* (2004) has been extended later on in Pueyo *et al.* (2008) to include beat-to-beat variations of QT dependency on HR, i.e. to account for possibly different adaptation characteristics along a recording of one and the same subject. Accordingly, both the linear and nonlinear subsystems used to model the QT/RR relationship are considered to be time variant in that case. The input response of the time-variant FIR filter is $\mathbf{h}(k) = [h_0(k) \dots h_{N-1}(k)]$, while the nonlinear function is approximated by a P th-order Taylor expansion in a neighbourhood of each $\overline{\text{RR}}$ measurement: $y_{\text{QT}}(k) = g(z_{\overline{\text{RR}}}(k), \mathbf{a}(k)) + v(k) = \mathbf{a}^T(k)z_{\overline{\text{RR}}}(k) + v(k)$, where $z_{\overline{\text{RR}}}(k) = \left[1 \quad z_{\overline{\text{RR}}}(k) \quad \dots \quad z_{\overline{\text{RR}}}^P(k) \right]^T$.

The averaged $\overline{\text{RR}}$ measurement is computed as $z_{\overline{\text{RR}}}(k) = \mathbf{h}^T(k)\mathbf{x}_{\text{RR}}(k)$, and the Taylor coefficients are $\mathbf{a}(k) = [a_0(k) \dots a_P(k)]^T$. An adaptive approach based on the Kalman filter is used to simultaneously estimate all of the system parameters, independently for each recording. Using this proposed methodology, it has been corroborated that QT hysteresis can range from just a few seconds in certain episodes of the recording with stable HR to several minutes in episodes of large HR changes.

The clinical value of investigating QT interval adaptation to HR has been shown in Schwartz *et al.* (1995), where insufficient QT adaptation after HR accelerations was found to be one possible factor explaining why, under stress conditions, patients with LQTS type 2 (reduced I_{Kr} kinetics) are at high risk of arrhythmic complications. In another study with LQTS patients, hysteresis of the RT interval (used instead of the QT interval) during exercise and recovery was shown to be much more marked in LQTS patients than in unaffected family members and control subjects (Krahn *et al.* 1997). Grom *et al.* studied the QT interval response after conversion from atrial fibrillation (AF) to sinus rhythm and, additionally, after a fall/increase in paced atrial rate (Grom *et al.* 2005). They reasoned why an inappropriately long QT interval in the onset of VT may degenerate into VF and why an inappropriately short QT after AF conversion can facilitate re-entrant and polymorphic tachyarrhythmias. Fossa *et al.* proposed biomarkers derived from the dynamic QT-RR analysis performed in their animal model, and suggested that, after appropriate adjustment, they could be useful in the future for arrhythmic risk prediction in humans (Fossa *et al.* 2006). Smetana *et al.* investigated 24-hour Holter recordings of post-MI patients randomized to treatment with placebo or amiodarone, who were followed up for a mean time of 2 years (Smetana *et al.* 2004a,b). They used the method described in Pueyo *et al.* (2004) and proposed novel risk markers derived from the analysis of QT adaptation to HR changes. They concluded that QT/HR analysis can be used to prospectively assess the prophylactic efficacy of class III antiarrhythmic drugs.

(b) QT variability

Despite HR being a major determinant of the QT interval, the contribution of other factors to QT modulation has been suggested to be also important from the clinical point of view. It is known that the ANS acts on both the SA node and the ventricular myocardium. Its influence on the SA node provokes changes in HR, which, in turn, affect the QT interval. On the other hand, the direct ANS action on the ventricular myocardium alters repolarization and, thus, the QT interval.

Evaluation of direct and indirect influences of ANS activity on QT may add to the understanding of arrhythmia susceptibility. The most extended approach in the literature to quantify temporal repolarization variability from the surface ECG is by measuring beat-to-beat fluctuations of the QT interval either in the time or the frequency domain, so-called QT variability (QTV). Many authors evaluate QTV after adjusting it by HR variability (HRV), thus providing a measurement of rate-independent QT variations or, in other words, of the extent of direct ANS influence on the ventricles. Several methods have been proposed to quantify QTV. In *Berger et al. (1997)*, QT variations out of proportion to HR variations were assessed by considering the following log-ratio index:

$$\text{QTVI} = \log \left[\frac{\text{QT}_v / \text{QT}_m^2}{\text{HR}_v / \text{HR}_m^2} \right], \quad (5.3)$$

where QT_m and QT_v denote the mean and variance of the QT series, and HR_m and HR_v denote the mean and variance of the HR series, respectively. In *Cuomo et al. (2004)*, QTV was evaluated in the time domain by calculating standard indices, such as SDNN, RMSSD or pNN50, applied to the QT series; also, QTV was quantified in the frequency domain by estimating QT power spectral density and computing its total power as well as the power in different frequency bands. Other methodologies have been proposed to assess variations in either shape or duration of ECG repolarization, thus generalizing the concept of QTV. Specifically, in *Burattini & Zareba (1999)*, variability of repolarization morphology through measurement of correlation between repolarization waves of consecutive beats was computed; in *Couderc et al. (1999)*, a wavelet-based method was proposed to quantify repolarization variability in both amplitude and time; in *Perkiömäki et al. (2002)*, time-domain measures quantifying variability of the QT interval and T_c were computed.

Another possibility to investigate repolarization variability is by using parametric modelling, as in *Porta et al. (1998)* for RT variability (RTV) or in *Almeida et al. (2006)* for QTV. The use of RT instead of QT avoids the need to determine the end of the T wave, which is usually considered to be problematic. However, owing to the fact that the RT interval is shorter than the QT interval, its variability is much reduced and, more importantly, the information provided by RTV and QTV has been shown to be different in certain populations, such as in patients with cardiovascular diseases (*Yeragani et al. 2007*). In relation to this, recent studies in the literature have shown that the interval between the apex and the end of the T wave possesses variability that is independent from HR and which can provide clinically useful information to be used for arrhythmic risk stratification (*Castro-Hevia et al. 2006*). The methodology described in *Almeida et al. (2006)* and *Porta et al. (1998)* considers a linear parametric model to quantify the interactions between QTV (or RTV) and HRV. It should be noted that the proposed model is only applicable under steady-state conditions, when just small variations around QT and RR means are expected. Consequently, the type of environments for analysis is substantially different from that considered in §5a, in which QT interval adaptation was investigated after possibly large HR changes. Identification of model parameters was performed in *Almeida et al. (2006)*, from which QTV fractions correlated and uncorrelated with HRV were quantified. On short-term recordings of healthy subjects, it was found that as much as 40 per cent of QTV was not related to HRV. Nevertheless, this result

does not imply that no physiological relationship exists between that QTV fraction and HR, since a linear relationship between them was assumed in the model, thus excluding possible nonlinear effects.

Increased repolarization variability has been reported under a variety of disease conditions that predispose to arrhythmic complications, such as: patients with dilated cardiomyopathy and patients with hypertrophic cardiomyopathy (Berger *et al.* 1997; Cuomo *et al.* 2004); during ischaemic episodes in ambulatory recordings of patients from the European ST–T database and in resting ECGs of patients with effort angina pectoris (Murabayashi *et al.* 2002); and patients with LQTS, in which elevated variability was found in both repolarization duration and shape (Burattini & Zareba 1999; Couderc *et al.* 1999; Perkiömäki *et al.* 2002).

Increased repolarization variability has also been documented to be predictive of arrhythmic complications. In a study with patients presenting for electrophysiological testing, significantly higher QTVI values were found in the subgroup of those who had aborted SCD or documented VF (Atiga *et al.* 1998). This was true both around the time of arrhythmic events and in advance of them. In Kudaiberdieva *et al.* (2003), recordings of post-MI patients were analysed and increased QTVI was shown to be an indicator of risk for developing arrhythmic events (VT or VF), the performance of QTVI being particularly strong when combined with other non-invasive markers such as late potentials. In Couderc *et al.* (2007), association between increased repolarization variability and risk for VT/VF was shown in post-MI patients with severe left ventricular dysfunction.

(c) *T-wave alternans*

TWA, or repolarization alternans, is a consistent beat-to-beat alternating change in the amplitude or morphology of the ST–T complex. While visible TWA had been occasionally reported since the beginning of the twentieth century, it is in the last two decades that signal processing techniques have allowed the detection and quantification of subtle TWA at the level of several microvolts (Martínez & Olmos 2005). The results provided by these new tools revealed that TWA is a common phenomenon associated with electrical instability and propensity to ventricular arrhythmia in cardiac conditions such as LQTS, myocardial ischaemia, MI, dilated cardiomyopathy or congestive heart failure. The presence of TWA has been widely validated as an index of SCD. A review of clinical results can be found in Narayan (2006b).

Elevated HR is needed in most patients to elicit TWA. Therefore, HR must be increased in a controlled way to obtain TWA-related risk indices (usually by pacing, or most commonly during exercise or pharmacological stress tests). Interestingly, unspecific TWA has also been reported in healthy subjects at high HRs (Turitto *et al.* 2001). Therefore, TWA must appear at HRs lower than 110–115 bpm to be considered as an index of susceptibility to SCD. Verrier *et al.* (2003) were able to identify patients at risk of SCD on spontaneous rhythm during ambulatory ECG recordings, opening the interesting possibility of ambulatory TWA testing.

TWA analysis can be seen as a combined detection–estimation problem (Martínez & Olmos 2005). The most relevant information to be found is whether TWA is present or not (i.e. a detection problem), but measurement of TWA magnitude (an estimation problem) may also be relevant. In fact, while most

studies use the presence of TWA as a clinical index, regardless of its magnitude, it has recently been shown that susceptibility to SCD is higher with increasing TWA magnitude (Klingenhöben *et al.* 2005). For TWA measurement, the TWA wave, i.e. the difference between the ST–T complexes in the odd- and even-beat patterns must be estimated and quantified in microvolts. Variations in this wave's magnitude can be observed in three dimensions: (i) the localization of TWA within repolarization interval, (ii) the temporal evolution of TWA, and (iii) the spatial distribution among the recorded leads. The distribution of TWA within the ST–T complex is usually disregarded, as the TWA waveform is integrated to obtain a global measurement for the whole ST–T complex. However, some authors have quantified the localization of TWA. Early TWA has been associated with acute ischaemia, even if different temporal distributions have been noted as a function of the occluded artery (Martínez *et al.* 2006). Later TWA has been identified in patients inducible for arrhythmia in ischaemia-free conditions (Narayan & Smith 1999).

Owing to its transient and episodic nature, TWA must be quantified in short excerpts, using a window with a fixed width in beats. Temporal changes of TWA magnitude can be tracked by shifting that window. The TWA time course is usually related with HR changes. In stress tests, a set of rules involving the onset HR and episode duration has been used to decide the result of the TWA test (Bloomfield *et al.* 2002). In the setting of ischaemia induced by coronary angioplasty, the relation between the time course of TWA and the timing of the artery occlusion has recently been characterized (Martínez *et al.* 2006). However, at present, whether temporal patterns in TWA can be clinically useful for risk stratification is unknown (Narayan 2006a). Finally, the distribution of TWA in the recorded leads has been shown to depend on the myocardium region responsible for TWA, with the greatest magnitude measured in leads overlying diseased regions during acute ischaemia (Martínez *et al.* 2006) and in post-MI patients (Narayan *et al.* 2006). These results suggest that spatial information could be used to improve the risk stratification power of TWA.

For TWA analysis, we can define a simple model for the i th ST–T complex of the l th lead as

$$x_{i,l}(n) = s_{i,l}(n) + \frac{1}{2} a_{i,l}(n)(-1)^i + v_{i,l}(n), \quad n = 0, \dots, N - 1, \quad (5.4)$$

where $s_{i,l}(n)$ is the background ST–T complex; $a_{i,l}(n)$ is the alternant wave; and $v_{i,l}(n)$ is the noise. Assuming that both $s_{i,l}(n)$ and $a_{i,l}(n)$ have a smooth beat-to-beat variation, the background ST–T complex can be easily cancelled by taking the difference between consecutive beats $y_{i,l}(n) = x_{i,l}(n) - x_{i-1,l}(n)$, which can be modelled as $y_{i,l}(n) = a_{i,l}(n)(-1)^i + w_{i,l}(n)$, with $w_{i,l}(n) = v_{i,l}(n) - v_{i-1,l}(n)$.

Analysis can be performed in a window of M consecutive beats, where the TWA wave $a_{i,l}(n)$ is assumed unaltered with i . This window must be conveniently shifted to cover the entire signal. For each position of the window, e.g. centred at j th beat, it must be decided whether TWA is absent ($a_{j,l}(n) = 0$ for every n) or present ($a_{j,l}(n) \neq 0$) by comparing a detection statistic $Z_{j,l}$ measuring the significance of TWA in the data with a threshold. Additionally, the analysis usually provides an estimate, $\hat{a}_{j,l}(n)$, of the alternant wave at each lead. This estimate informs about TWA amplitude and how it is distributed within the repolarization interval. The magnitude of TWA in the whole ST–T complex is

usually described as a global alternans voltage $A_{j,l}$, e.g. the r.m.s. of $a_{j,l}(n)$. The variation of $Z_{j,l}$ and $A_{j,l}$ in the beat and lead indices acquaints, respectively, for time course and spatial distribution of TWA.

A comprehensive review of the methods proposed for TWA analysis can be found in [Martínez & Olmos \(2005\)](#). They concluded that all the TWA analysis schemes that have been used in the clinical literature are based on or are equivalent to one of these three signal processing techniques: the short-term Fourier transform (STFT); sign-change counting; and nonlinear filtering.

The first class of methods is characterized by windowed Fourier analysis applied to each of the beat-to-beat series of synchronized samples within the ST–T complex. The TWA component is obtained by evaluating the STFT at the alternans frequency (i.e. 0.5 cycles per beat), obtaining

$$z_{j,l}(n) = \sum_{i=-\infty}^{\infty} x_{i,l}(n)w(i-j)(-1)^i, \quad (5.5)$$

where $z_{j,l}(n)$ reflects the TWA component. As shown in [Martínez & Olmos \(2005\)](#), this process is equivalent to a linear high-pass filtering of the beat-to-beat series. The width of the window $w(i)$ defines the stationarity requirement for the signal and the classical trade-off between accuracy and tracking ability. The main drawback of this approach is the sensitivity to impulsive artefacts or outliers in the beat-to-beat series, as a consequence of the linearity of STFT. Of the methods in this class, the most widely used is the spectral method ([Rosenbaum et al. 1994](#)), which also uses other frequency bins of the STFT to estimate the noise content and to define a *TWA ratio* that is compared with threshold for detection. This makes the method insensitive to changes in the noise level, reducing the risk of false alarms.

The second class refers to methods based on sign changes of the detrended beat-to-beat series ([Martínez & Olmos 2005](#)). Although insensitive to impulsive artefacts, these methods are very sensitive to the presence of high-amplitude non-alternant components. Another notable drawback is the loss of TWA amplitude information.

The third class includes two recently described methods that use nonlinear time-domain approaches instead of the linear Fourier-based techniques. The *modified moving average method* recursively estimates the odd and even ST–T complex patterns using a moving average whose updating term is modified by a nonlinear limiting function ([Nearing & Verrier 2002](#)). TWA at each beat is defined as the difference between the two estimated patterns. When the signal variations are smooth, the method works linearly and is equivalent to the STFT-based methods. When abrupt changes, artefacts or abnormal beats occur, the nonlinear function minimizes their effect on the TWA estimate. However, the method does not adapt to the noise level, which makes it sensitive to noise-level changes.

The Laplacian likelihood ratio is a statistical model-based approach for TWA, where the *generalized likelihood ratio test* (GLRT) and the *maximum likelihood estimate* (MLE) are used, respectively, for TWA detection and estimation ([Martínez & Olmos 2005](#)). A signal model similar to (5.4) was considered, where the noise was assumed to have a zero-mean Laplacian distribution with unknown variance. The use of a heavy-tailed distribution makes the methodology robust to outliers or abrupt changes in the beat-to-beat series. In fact, the MLE is the

median-filtered demodulated beat-to-beat series

$$\hat{a}_{j,l}(n) = \text{median}\{y_{i,l}(n)(-1)^i\}_{i \in W_j}, \quad (5.6)$$

where W_j is the analysis window centred at beat j . The GLRT statistic is

$$Z_{j,l} = \frac{\sqrt{2}}{\hat{\sigma}_{j,l}} \sum_{n=0}^{N-1} \left(\sum_{i \in W_j} |y_{i,l}(n)| - |y_{i,l}(n) - \hat{a}_{j,l}(n)(-1)^i| \right), \quad (5.7)$$

where

$$\hat{\sigma}_{j,l} = \frac{1}{\sqrt{2NL}} \sum_{n=0}^{N-1} \sum_{i \in W_j} |y_{i,l}(n) - \hat{a}_{j,l}(n)(-1)^i|$$

is an estimate of the noise level. It is easy to test that the probability of false alarm in this detection scheme is insensitive to changes in the noise conditions.

Although all these methods work on a lead-by-lead basis, recent results using a multilead PCA-based strategy suggest that improved detection and estimation performance can be obtained by jointly processing all the available leads, taking profit of the different interlead correlations of TWA and noise components (Monasterio & Martínez 2007). The clinical relevance of these results is still to be determined.

6. Conclusions

Using the ECG signal, different proarrhythmic risk markers have been proposed in the literature, some of them with limited ability to predict risk, and others promising but with its clinical utility yet to be confirmed. In this paper, we provide a review of techniques developed to investigate cardiac repolarization from the surface ECG. Techniques are divided into two categories: on the one hand, those that measure spatial dispersion of repolarization (some based on interval repolarization durations: QT dispersion, T-wave width or the distance from the peak to the end of the T wave; and others based on T-wave morphology: total cosine R-to-T descriptor, the morphology dispersion index or the T-wave residuum) and, on the other hand, those measuring temporal dispersion of repolarization (analysis of QT interval dynamics after HR changes, beat-to-beat variability of the QT interval and TWA). For the reviewed techniques, a description of their value for risk stratification is presented. Emphasis is placed on the fact that some of the reported indices have been well validated as indices of mortality, others of arrhythmic death, while others are less well validated.

This study was supported by CICYT TEC2007-68076-C02-02, and in part by Diputación General de Aragón (DGA), Spain, through Grupos Consolidados GTC ref:T30.

References

- Acar, B., Yi, G., Hnatkova, K. & Malik, M. 1999 Spatial, temporal and wavefront direction characteristics of 12-lead T-wave morphology. *Med. Biol. Eng. Comput.* **37**, 574–584. (doi:10.1007/BF02513351)

- Ahnve, S. & Vallin, H. 1982 Influence of heart rate and inhibition of autonomic tone on the QT interval. *Circulation* **65**, 435–439.
- Akar, F. G. & Tomaselli, G. F. 2004 Ionic mechanisms of cardiac arrhythmias. *Drug Discov. Today. Dis. Mech.* **1**, 23–30. (doi:10.1016/j.ddmec.2004.08.005)
- Almeida, R., Gouveia, S., Rocha, A. P., Pueyo, E., Martínez, J. P. & Laguna, P. 2006 QT variability and HRV interactions in ECG: quantification and reliability. *IEEE Trans. Biomed. Eng.* **53**, 1317–1329. (doi:10.1109/TBME.2006.873682)
- Arini, P., Martínez, J. P. & Laguna, P. 2006 Analysis of T-wave width during severe ischemia generated by percutaneous transluminal coronary angioplasty. *Proc. Comput. Cardiol.* **33**, 713–716.
- Arini, P., Bertrán, G., Valverde, E. & Laguna, P. 2008 T-wave width as an index for quantification of ventricular repolarization dispersion: evaluation in an isolated rabbit heart model. *Biomed. Signal Process. Control* **3**, 67–77. (doi:10.1016/j.bspc.2007.10.001)
- Atiga, W. L., Calkins, H., Lawrence, J. H., Tomaselli, G. F., Smith, J. F. & Berger, R. D. 1998 Beat-to-beat repolarization lability identifies patients at risk for sudden cardiac death. *J. Cardiovasc. Electrophysiol.* **9**, 899–908. (doi:10.1111/j.1540-8167.1998.tb00130.x)
- Badilini, F., Blanche, P. M., Fayn, J., Forlini, M. C., Rubel, P. & Coumel, P. 1995 Relationship between 12-lead ECG QT dispersion and 3-D-ECG repolarization loop. *Proc. Comput. Cardiol.* **22**, 785–788.
- Berger, R. D., Kasper, E. K., Baughman, K. L., Marban, E., Calkins, H. & Tomaselli, G. F. 1997 Beat-to-beat QT interval variability: novel evidence for repolarization lability in ischemic and nonischemic dilated cardiomyopathy. *Circulation* **96**, 1557–1565.
- Bloomfield, D. M., Hohnloser, S. H. & Cohen, R. J. 2002 Interpretation and classification of microvolt T-wave alternans tests. *J. Cardiovasc. Electrophysiol.* **13**, 502–512. (doi:10.1046/j.1540-8167.2002.00502.x)
- Burattini, L. & Zareba, W. 1999 Time-domain analysis of beat-to-beat variability of repolarization morphology in patients with ischemic cardiomyopathy. *J. Electrocardiol.* **32**, 166–172. (doi:10.1016/S0022-0736(99)90075-4)
- Carmeliet, E. 2006 Action potential duration, rate of stimulation, and intracellular sodium. *J. Cardiovasc. Electrophysiol.* **17**, S2–S7. (doi:10.1111/j.1540-8167.2006.00378.x)
- Castells, F., Laguna, P., Sörnmo, L., Bollmann, A. & Millet, J. 2007 Principal component analysis in ECG signal processing. *EURASIP J. Adv. Signal Process.* **2007**, 1–21. (doi:10.1155/2007/74580)
- Castro-Hevia, J., Antzelevitch, C., Tornés-Bárzaga, F., Dorantes-Sánchez, M., Dorticós-Balea, F., Zayas-Molina, R., Quiñones-Pérez, M. A. & Fayad-Rodríguez, Y. 2006 Tpeak-Tend and Tpeak-Tend dispersion as risk factors for ventricular tachycardia/ventricular fibrillation in patients with the Brugada syndrome. *J. Am. Coll. Cardiol.* **47**, 1828–1834. (doi:10.1016/j.jacc.2005.12.049)
- Couderc, J. P., Zareba, W., Burattini, L. & Moss, A. J. 1999 Beat-to-beat repolarization variability in LQTS patients with the SCN5A sodium channel gene mutation. *Pacing Clin. Electrophysiol.* **22**, 1581–1592. (doi:10.1111/j.1540-8159.1999.tb00376.x)
- Couderc, J. P., Zareba, W., McNitt, S., Maison-Blanche, P. & Moss, A. J. 2007 Repolarization variability in the risk stratification of MADIT II patients. *Europace* **9**, 717–723. (doi:10.1093/europace/eum131)
- Coumel, P. 1993 Cardiac arrhythmias and the autonomic nervous system. *J. Cardiovasc. Electrophysiol.* **4**, 338–355. (doi:10.1111/j.1540-8167.1993.tb01235.x)
- Cuomo, S., Marciano, F., Migaux, M. L., Finizio, F., Pezzella, E., Losi, M. A. & Betocchi, S. 2004 Abnormal QT interval variability in patients with hypertrophic cardiomyopathy: can syncope be predicted? *J. Electrocardiol.* **37**, 113–119. (doi:10.1016/j.jelectrocard.2004.01.010)
- Day, C. P., McComb, J. M. & Campbell, R. W. 1990 QT dispersion: an indication of arrhythmia risk in patients with long QT intervals. *Br. Heart J.* **63**, 342–344. (doi:10.1136/hrt.63.6.342)
- Dessertenne, F. 1966 La tachycardie ventriculaire à deux foyers opposés variables. *Arch Mal Coeur Vaiss* **59**, 263–272.

- di Bernado, D. & Murray, A. 2000 Computer model for study of cardiac repolarization. *J. Cardiovasc. Electrophysiol.* **11**, 895–899. (doi:10.1111/j.1540-8167.2000.tb00069.x)
- Fossa, A. A., Wisialowski, T. & Crimin, K. 2006 QT prolongation modifies dynamic restitution and hysteresis of the beat-to-beat QT–TQ interval relationship during normal sinus rhythm under varying states of repolarization. *J. Pharmacol. Exp. Ther.* **316**, 498–506. (doi:10.1124/jpet.105.095471)
- Fuller, M., Sándor, G., Punske, B., Taccardi, B., MacLeod, R., Ershler, P., Green, L. & Lux, R. 2000 Estimates of repolarization dispersion from electrocardiographic measurements. *Circulation* **102**, 685–691.
- Gima, K. & Rudy, Y. 2002 Ionic current basis of electrocardiographic waveforms: a model study. *Circ. Res.* **90**, 889–896. (doi:10.1161/01.RES.0000016960.61087.86)
- Grom, A., Faber, T. S., Brunner, M., Bode, C. & Zehender, M. 2005 Delayed adaptation of ventricular repolarization after sudden changes in heart rate due to conversion of atrial fibrillation. A potential risk factor for proarrhythmia? *Europace* **7**, 113–121. (doi:10.1016/j.eupc.2005.01.001)
- Hondeghem, L. M., Carlsson, L. & Duker, G. 2001 Instability and triangulation of the action potential predict serious proarrhythmia, but action potential duration prolongation is antiarrhythmic. *Circulation* **103**, 2004–2013.
- Klingenheben, T., Ptaszinski, P. & Hohnloser, S. H. 2005 Quantitative assessment of microvolt T-wave alternans in patients with congestive heart failure. *J. Cardiovasc. Electrophysiol.* **16**, 620–624. (doi:10.1111/j.1540-8167.2005.40708.x)
- Kors, J., van Herpen, G. & van Bemmel 1999 QT dispersion as an attribute of T-loop morphology. *Circulation* **99**, 1458–1463.
- Krahn, A. D., Klein, G. J. & Yee, R. 1997 Hysteresis of the RT interval with exercise: a new marker for the long-QT syndrome? *Circulation* **96**, 1551–1556.
- Kudaiberdieva, G., Gorenek, B., Goktekin, O., Cavusoglu, Y., Birdane, A., Unalir, A., Ata, N. & Timuralp, B. 2003 Combination of QT variability and signal-averaged electrocardiography in association with ventricular tachycardia in postinfarction patients. *J. Electrocardiol.* **36**, 17–24. (doi:10.1054/jelc.2003.50003)
- Kuo, C. S. & Surawicz, B. 1976 Ventricular monophasic action potential changes associated with neurogenic T wave abnormalities and isoproterenol administration in dogs. *Am. J. Cardiol.* **38**, 170–177. (doi:10.1016/0002-9149(76)90145-4)
- Langley, P., Bernardo, D. & Murray, A. 2002 Quantification of T wave shape changes following exercise. *Pacing Clin. Electrophysiol.* **25**, 1230–1234. (doi:10.1046/j.1460-9592.2002.01230.x)
- Lau, C. P., Freedman, A. R., Fleming, S., Malik, M., Camm, A. J. & Ward, D. E. 1988 Hysteresis of the ventricular paced QT interval in response to abrupt changes in pacing rate. *Cardiovasc. Res.* **22**, 67–72. (doi:10.1093/cvr/22.1.67)
- Lawrence, C. L., Pollard, C. E., Hammond, T. G. & Valentin, J. P. 2005 Nonclinical proarrhythmia models: predicting Torsades de Pointes. *J. Pharmacol. Toxicol. Methods* **52**, 46–59. (doi:10.1016/j.vascn.2005.04.011)
- Lewis, M. J. & Short, A. L. 2006 Hysteresis of electrocardiographic depolarization–repolarization intervals during dynamic physical exercise and subsequent recovery. *Physiol. Meas.* **27**, 191–201. (doi:10.1088/0967-3334/27/2/009)
- Macfarlane, P. W., McLaughlin, S. C. & Rodger, J. C. 1998 Influence of lead selection and population on automated measurement of QT dispersion. *Circulation* **98**, 2160–2167.
- Malfatto, G., Beria, G., Sala, S., Bonazzi, O. & Schwartz, P. J. 1994 Quantitative analysis of T wave abnormalities and their prognostic implications in the idiopathic long QT syndrome. *J. Am. Coll. Cardiol.* **23**, 296–301.
- Malik, M. 2001 Problems of heart rate correction in assessment of drug-induced QT interval prolongation. *J. Cardiovasc. Electrophysiol.* **12**, 411–420. (doi:10.1046/j.1540-8167.2001.00411.x)
- Malik, M. 2004 Errors and misconceptions in ECG measurement used for the detection of drug induced QT-interval prolongation. *J. Electrocardiol.* **37**, 25–33. (doi:10.1016/j.jelectrocard.2004.08.005)

- Malik, M., Acar, B., Gang, Y., Yap, Y. G., Hnatkova, K. & Camm, A. 2000 QT dispersion does not represent electrocardiographic interlead heterogeneity of ventricular repolarization. *J. Cardiovasc. Electrophysiol.* **11**, 835–843. (doi:10.1111/j.1540-8167.2000.tb00061.x)
- Malmivuo, J. & Plonsey, R. 1995 *Principles and applications of bioelectric and biomagnetic fields*. New York, NY: Oxford University Press.
- Martínez, J. P. & Olmos, S. 2005 Methodological principles of T wave alternans analysis. A unified framework. *IEEE Trans. Biomed. Eng.* **52**, 599–613. (doi:10.1109/TBME.2005.844025)
- Martínez, J. P., Almeida, R., Olmos, S., Rocha, A. P. & Laguna, P. 2004 A wavelet-based ECG delineator: evaluation on standard databases. *IEEE Trans. Biomed. Eng.* **51**, 570–581. (doi:10.1109/TBME.2003.821031)
- Martínez, J. P., Olmos, S., Wagner, G. & Laguna, P. 2006 Characterization of repolarization alternans during ischemia: time-course and spatial analysis. *IEEE Trans. Biomed. Eng.* **53**, 701–711. (doi:10.1109/TBME.2006.870233)
- Martínez, J. P., Laguna, P., Olmos, S., Pahlm, O., Pettersson, J. & Sörnmo, L. 2007 Assessment of QT-measurement accuracy using the 12-lead electrocardiogram derived from EASI leads. *J. Electrocardiol.* **40**, 172–179. (doi:10.1016/j.jelectrocard.2006.08.089)
- Monasterio, V. & Martínez, J. P. 2007 A multilead approach to T-wave alternans detection combining principal component analysis and the Laplacian likelihood ratio method. *Proc. Comput. Cardiol.* **34**, 5–8.
- Murabayashi, T., Fetits, B., Kass, D., Nevo, E., Gramatikov, B. & Berger, R. D. 2002 Beat-to-beat QT interval variability associated with acute myocardial ischemia. *J. Electrocardiol.* **35**, 19–25. (doi:10.1054/jelc.2002.30250)
- Narayan, S. M. 2006a Pathophysiology guided T-wave alternans measurement. In *Fundamental algorithms* (eds G. D. Clifford, F. Azuaje & P. E. McSharry), pp. 197–214. Norwood, MA: Artech House Publishing.
- Narayan, S. M. 2006b T-wave alternans and the susceptibility to ventricular arrhythmias. *J. Am. Coll. Cardiol.* **47**, 269–281. (doi:10.1016/j.jacc.2005.08.066)
- Narayan, S. M. & Smith, J. M. 1999 Differing rate dependence and temporal distribution of repolarization alternans in patients with and without ventricular tachycardia. *J. Cardiovasc. Electrophysiol.* **10**, 61–71. (doi:10.1111/j.1540-8167.1999.tb00643.x)
- Narayan, S. M., Smith, J. M., Lindsay, B. D., Cain, M. E. & Dávila-Román, V. G. 2006 Relation of T-wave alternans to regional left ventricular dysfunction and eccentric hypertrophy secondary to coronary heart disease. *Am. J. Cardiol.* **97**, 775–780. (doi:10.1016/j.amjcard.2005.09.127)
- Nearing, B. D. & Verrier, R. L. 2002 Modified moving average analysis of T-wave alternans to predict ventricular fibrillation with high accuracy. *J. Appl. Physiol.* **92**, 541–549.
- Okin, P. M., Devereux, R. B., Howard, B. V., Fabsitz, R. R., Lee, E. T. & Welty, T. K. 2000 Assessment of QT interval and QT dispersion for prediction of all-cause and cardiovascular mortality in American Indians: the strong heart study. *Circulation* **101**, 61–66.
- Padrini, R., Speranza, G., Nollo, G., Bova, S., Piovan, D., Antolini, R. & Ferrari, M. 1997 Adaptation of the QT interval to heart rate changes in isolated perfused guinea pig heart: influence of amiodarone and D-sotalol. *Pharmacol. Res.* **35**, 409–416. (doi:10.1006/phrs.1997.0152)
- Pastore, J. M., Girouard, S. D., Laurita, K. R., Akar, F. G. & Rosenbaum, D. S. 1999 Mechanism linking T-wave alternans to the genesis of cardiac fibrillation. *Circulation* **99**, 1385–1394.
- Perkiömäki, J. S., Zareba, W., Nomura, A., Andrews, M., Kaufman, E. S. & Moss, A. J. 2002 Repolarization dynamics in patients with long QT syndrome. *J. Cardiovasc. Electrophysiol.* **13**, 651–656. (doi:10.1046/j.1540-8167.2002.00651.x)
- Porta, A., Baselli, G., Caiani, E., Malliani, A., Lombardi, F. & Cerutti, S. 1998 Quantifying electrocardiogram RT-RR variability interactions. *Med. Biol. Eng. Comput.* **36**, 27–34. (doi:10.1007/BF02522854)
- Priori, S., Mortara, D., Napolitano, C., Diehl, L., Paganini, V., Cantù, F., Cantù, G. & Schwartz, P. 1997 Evaluation of the spatial aspects of T wave complexity in the long-QT syndrome. *Circulation* **96**, 3006–3012.

- Pueyo, E., Smetana, P., Caminal, P., de Luna, A. B., Malik, M. & Laguna, P. 2004 Characterization of QT interval adaptation to RR interval changes and its use as a risk-stratifier of arrhythmic mortality in amiodarone-treated survivors of acute myocardial infarction. *IEEE Trans. Biomed. Eng.* **51**, 1511–1520. (doi:10.1109/TBME.2004.828050)
- Pueyo, E., Malik, M. & Laguna, P. 2008 A dynamic model to characterize beat-to-beat adaptation of repolarization to heart rate changes. *Biomed. Signal Process. Control* **3**, 29–43. (doi:10.1016/j.bspc.2007.09.005)
- Rosenbaum, D. S., Jackson, L. E., Smith, J. M., Garan, H., Ruskin, J. N. & Cohen, R. J. 1994 Electrical alternans and vulnerability to ventricular arrhythmias. *N. Engl. J. Med.* **330**, 235–241. (doi:10.1056/NEJM199401273300402)
- Sarma, J. S., Venkataraman, S. K., Samant, D. R. & Gadgil, U. 1987 Hysteresis in the human RR-QT relationship during exercise and recovery. *Pacing Clin. Electrophysiol.* **10**, 485–491. (doi:10.1111/j.1540-8159.1987.tb04510.x)
- Schwartz, P. J. *et al.* 1995 Long QT syndrome patients with mutations of the SCN5A and HERG genes have differential responses to Na⁺ channel blockade and to increases in heart rate. Implications for gene-specific therapy. *Circulation* **92**, 3381–3386.
- Simón, F., Laguna, P. & Pueyo, E. 2007 Study of the dynamic relationship between T wave morphology and heart rate during ischemia. *Proc. Comput. Cardiol.* **34**, 297–300.
- Smetana, P., Batchvarov, V. N., Hnatkova, K., Camm, A. J. & Malik, M. 2004a Ventricular gradient and nondipolar repolarization components increase at higher heart rate. *Am. J. Physiol. Heart Circ. Physiol.* **286**, 131–136. (doi:10.1152/ajpheart.00479.2003)
- Smetana, P., Pueyo, E., Hnatkova, K., Batchvarov, V., Laguna, P. & Malik, M. 2004b Individual patterns of dynamic QT/RR relationship in survivors of acute myocardial infarction and their relationship to antiarrhythmic efficacy of amiodarone. *J. Cardiovasc. Electrophysiol.* **15**, 1147–1154. (doi:10.1046/j.1540-8167.2004.04076.x)
- Smith, T. W. & Cain, M. E. 2006 Sudden cardiac death: epidemiologic and financial worldwide perspective. *J. Interv. Card. Electrophysiol.* **17**, 199–203. (doi:10.1007/s10840-006-9069-6)
- Sörnmo, L. & Laguna, P. 2005 *Biomedical signal processing in cardiac and neurological applications*. London, UK: Elsevier Academic Press.
- Turitto, G., Caref, E. B., El-Attar, G., Helal, M., Mohamed, A., Pedalino, R. P. & El-Sherif, N. 2001 Optimal target heart rate for exercise-induced T-wave alternans. *Ann. Noninv. Electrocardiol.* **6**, 123–128. (doi:10.1111/j.1542-474X.2001.tb00096.x)
- Verrier, R. L., Nearing, B. D., LaRovere, M. T., Pinna, G. D., Mittleman, M. A., Bigger, J. T. & Schwartz, P. J. 2003 Ambulatory electrocardiogram-based tracking of T wave alternans in postmyocardial infarction patients to assess risk of cardiac arrest or arrhythmic death. *J. Cardiovasc. Electrophysiol.* **14**, 705–711.
- Yap, Y. G. & Camm, A. J. 2003 Drug induced QT prolongation and Torsades de Pointes. *Heart* **89**, 1363–1372. (doi:10.1136/heart.89.11.1363)
- Yeragani, V. K., Berger, R., Desai, N., Bar, K. J., Chokka, P. & Tancer, M. 2007 Relationship between beat-to-beat variability of RT-peak and RT-end intervals in normal controls, patients with anxiety, and patients with cardiovascular disease. *Ann. Noninv. Electrocardiol.* **12**, 203–209. (doi:10.1111/j.1542-474X.2007.00162.x)
- Zabel, M., Lichtlen, P. R., Haverich, A. & Franz, M. 1998 Comparison of ECG variables of dispersion of ventricular repolarization with direct myocardial repolarization measurements in the humans heart. *J. Cardiovasc. Electrophysiol.* **9**, 1279–1284. (doi:10.1111/j.1540-8167.1998.tb00103.x)
- Zareba, W., Couderc, J. & Moss, A. 2000 Automatic detection of spatial and temporal heterogeneity of repolarization. In *Dispersion of ventricular repolarization* (eds S. B. Olsson, J. P. Amlie & S. Yuan), pp. 85–107. New York, NY: Futura Publishing.